

Numerical Modelling of the Thermal State of a Cylinder Head [†]

Delyan Petkov ¹ and Simeon Iliev ^{2,*}

¹ Department of Transport Engineering and Technologies, Technical University of Varna, 9000 Varna, Bulgaria; delyan.petkov@tu-varna.bg

² Department of Engines and Vehicles, University of Ruse, 7012 Ruse, Bulgaria

* Correspondence: spi@uni-ruse.bg; Tel.: +359-82888331

[†] Presented at the 6th International Conference on Communications, Information, Electronic and Energy Systems, 26–28 November 2025, Ruse, Bulgaria.

Abstract

The presented work is part of a comprehensive study exploring the feasibility of spark-ignited engines operating on fuels enhanced with additives derived from renewable sources. The investigation focuses on understanding how these alternative fuel mixtures influence engine performance and durability. In particular, attention was given to the thermal behavior of the cylinder head during engine operation with gasoline–ethanol blends. The cylinder head was selected for detailed analysis because it is one of the most thermally stressed components in the engine, directly exposed to combustion heat and pressure. Understanding its thermal state is crucial for assessing the impact of renewable fuel additives on engine reliability, efficiency, and emission characteristics. This study aims to provide insights into optimizing engine design and fuel formulation to accommodate sustainable fuel alternatives while maintaining or improving engine operation under varying conditions.

Keywords: gasoline engine; FEM; alternative fuels; engine simulation; heat transfer

1. Introduction

Understanding the thermal state of internal combustion engine components is crucial, particularly when there are alterations in the operational parameters or modifications to the engine design. This is especially relevant in the context of utilizing alternative fuels, such as gasoline–ethanol blends. If that is the case, it is the thermal condition of the cylinder head that serves as the key indicator for determining the necessary adjustments to the engine design in response to the changes in the type of the fuel.

Conducting purely experimental research to ascertain the temperature distribution across the cylinder head is inherently complex and often yields limited results. Proposed, therefore, in the present paper is a theoretical–experimental approach that leverages experimentally obtained temperature measurements at specific points to construct a comprehensive temperature field for the entire cylinder head. This is achieved through the utilization of a numerical model that simulates the thermal state of the cylinder head.

The numerical modelling draws upon data derived from a laboratory study examining the thermal conditions of cylinder heads, conducted by the Department of Transport Engineering and Technologies at the Technical University of Varna, as previously outlined in an earlier publication [1].

The 3D modelling was performed within the SolidWorks 2024 environment, which provides robust capabilities for analyzing mechanical and thermal stresses [2]. This platform features an extensive library of basic machine elements and a diverse array of materials,



Academic Editors: Teodor Iliev, Ivaylo Stoyanov and Grigor Mihaylov

Published: 15 January 2026

Corrected: 25 March 2026

Copyright: © 2026 by the authors.

Licensee MDPI, Basel, Switzerland.

This article is an open access article distributed under the terms and conditions of the [Creative Commons Attribution \(CC BY\)](https://creativecommons.org/licenses/by/4.0/) license.

each with specific properties. The volumetric representation of the shape of the cylinder head encompasses all intricacies of its design, as even tiniest geometric alterations can have a dramatic effect on the outcomes of stress and deformation analyses.

A widely accepted method for addressing problems related to stress and deformation is the Finite Element Method (FEM), a numerical network technique. The FEM involves approximating the solution of the continuously varying within the volume of the body quantity (temperature, displacement) to its discrete model [3]. The model is constructed through the use of an interpolating polynomial, capturing the variation in the target function within the confines of a finite element's volume, which is based on the function's values at the nodes along the element's edges [4]. To achieve this, the body must be fragmented into a sufficiently small set of elements, each with distinct geometric shapes -finite elements. In the context of heat conduction problems, the finite element method is employed [5]. Grounded in four years [6]. Law of heat conduction [7]. In addressing heat conduction issues, the FEM is employed, founded on Fourier's law of heat transfer.

2. Experimental Results

Numerical modelling is one of the effective approaches to extend the results of experimentally measured temperatures and gain a comprehensive view of the temperature field within the cylinder head.

The accuracy of the results is dependent upon the precision of the three-dimensional representation and the appropriate specification of the thermal boundary conditions. Implemented, in the proposed numerical model, are the first-kind boundary conditions (temperature values) and third-kind boundary conditions (parameters governing the convective heat exchange between the gas medium and the surfaces of the cylinder head: $(\alpha g.\text{avg} [W/(m^2.\text{deg})]$, and the resultant temperature $t_{g.res} [^{\circ}\text{C}]$).

The temperatures measured during laboratory experiments are directly incorporated into the numerical model as boundary conditions of the first kind.

Determining the third-kind boundary conditions directly can be quite challenging. An indirect approach is, therefore, adopted for their estimation. The initial values for these parameters are derived from the existing literature, and the subsequent adjustments are made based on the temperature readings at designated control points. It is at these specific locations, where the temperatures obtained from the numerical simulations are compared with those measured experimentally. Modifications to the boundary conditions are implemented until the temperature values from the experimental data and the numerical model converge or are sufficiently close.

To establish the variable parameters for the current study, a load characteristic mode was selected at 3000 min^{-1} , based on laboratory tests, with an open throttle position of 30%. Subject to these conditions, the engine Daewoo Lanos 1,4 cc (Daewoo Motor, Bupyeong, Republic of Korea) under examination demonstrates an effective power output of 25.2 kW. The fuel utilized in this experiment is standard gasoline blended with 20% ethanol. This specific operational mode is among the most frequently employed in automotive applications, where issues related to the thermal state of various engine components are commonly observed.

For each of the operational regimes under study, first-kind boundary conditions are applied to both external and internal surfaces, utilizing values obtained from laboratory measurements. These values are detailed in Tables 1 and 2.

The points, where temperatures t_1 through t_5 were recorded, are shown in Figure 1.

In the numerical model, the temperature readings correspond to the positions of the thermocouples used in the laboratory experiments. To ensure precision in measurements,

openings are “drilled” in the model at the exact locations of the thermocouples, allowing the samples to capture temperatures at the bottom of these holes (Figure 2).

Table 1. First-kind boundary conditions.

Pe, (KW)	t1, (°C)	t2, (°C)	t3, (°C)	t4, (°C)	t5, (°C)
19.20	55	94	89	85	79
25.20	60	95	90	86	82
33.90	64	101	95	90	88
38.40	71	104	99	92	90

Table 2. First-kind boundary conditions.

Cooling Space, (°C)	Intake Runners, (°C)	Exhaust Runners, (°C)
85	28	417
85	29	509
85	29	562
85	31	584

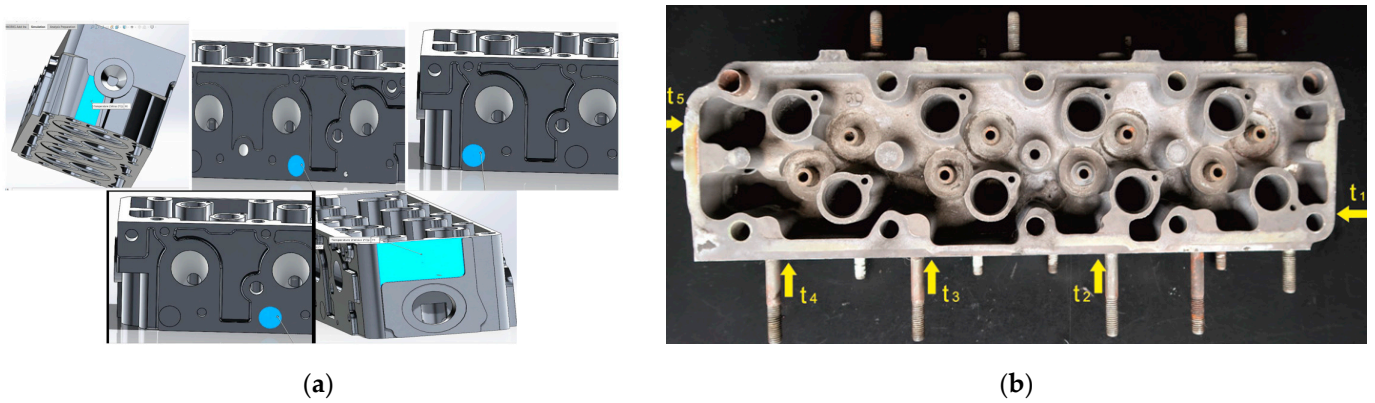


Figure 1. Points, where temperatures t1 through t5 were recorded: (a) SolidWorks model; (b) Cylinder Head.

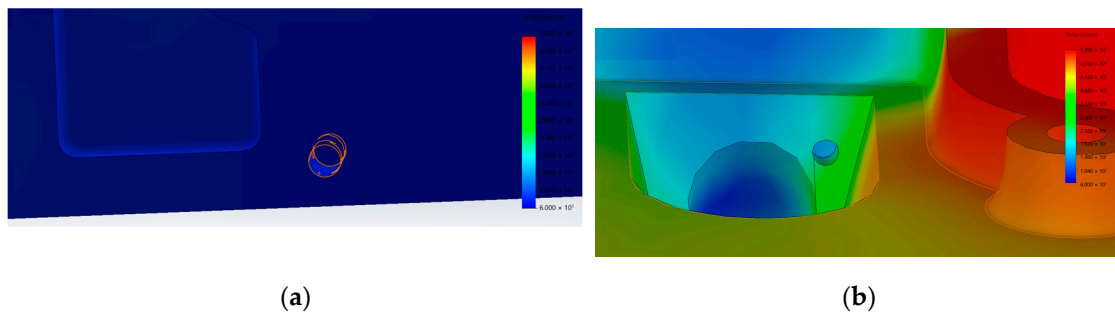


Figure 2. Locations of the thermocouples: (a) Thermocouple hole 4; (b) Thermocouple hole 1.

The material selected for the model is cast aluminium alloy containing 13% silicon, alloyed with copper and magnesium, as specified in the material catalogue of the SolidWorks 2024 software [6]. This choice of material closely matches that of the actual component used in the experimental study.

The parameters for convective heat transfer ($\alpha_{g.avg}$ [W/(m².deg)]) and the resultant temperature $t_{g.res}$ [°C]), which serve as boundary conditions of the third kind, are determined through an iterative process, involving successive approximations during the numerical experiment until the temperature values at the specified points of the calculated temperature field aligned closely with those measured by the thermocouples in the con-

tinuous monitoring system. The resulting parameters, thus obtained, in direct correlation with the effective power are presented in Tables 3 and 4.

Table 3. Correlation with the effective power.

Pe, (KW)	Pe, (MPa)	α , (W/m ² K)	Res t°	α , (W/m ² K)
19.20	0.55	249	900	85
25.20	0.72	285	1045	86
33.90	0.97	374	1395	90
38.40	1.10	392	1450	92

Table 4. Correlation with the effective power.

Res t°	Pe, (KW)	Pe, (MPa)	α , (W/m ² K)
800	19.20	0.55	249
850	25.20	0.72	285
1000	33.90	0.97	374
1030	38.40	1.10	392

The results acquired from the experiments have been compared with the measured temperatures obtained from the laboratory experiment, as presented in Tables 5–8. Displayed in that table is also the percentage difference between the measured and calculated temperature values. The iterative process of refining the boundary conditions can be continued to achieve even greater accuracy.

Table 5. Comparison of data from numerical and laboratory experiments.

Pe, (MPa)	Pe, (KW)	tc1	tc1 NE
0.549	19.20	149.2	151.2
0.720	25.20	152.1	154.5
0.969	33.90	172.3	173.8
1.097	38.40	176.6	177.2

Table 6. First-kind boundary conditions: NE-numerical experiment.

Δ [%]	tc2	tc2 NE	Δ (%)
1.32	146.3	145.5	0.55
1.55	149.8	148.8	0.67
0.86	168.2	166.4	1.07
0.34	172.5	171.3	0.70

Table 7. First-kind boundary conditions: NE-numerical experiment.

Pe, (Mpa)	Pe, (KW)	tc3	tc3 NE
0.549	19.20	91.8	93.2
0.720	25.20	95.8	96.4
0.969	33.90	104.7	105.7
1.097	38.40	106.1	107.7

The boundary conditions of the third kind, which pertained to the surfaces of the combustion chamber, are determined by the engine load.

One of the significant benefits of extending the laboratory results with numerical standards is the ability to evaluate the impact of the engine's mean effective pressure on the third-kind boundary conditions.

Table 8. First-kind boundary conditions: NE-numerical experiment.

Δ (%)	tc4	tc4 NE	Δ (%)
1.50	94.1	93.4	0.74
0.62	103.9	96.6	7.03
0.95	105.3	105.2	0.09
1.49	106.9	107.2	0.28

The graphical representations visualized in Figures 3–6 are constructed using the data provided in Tables 7 and 8. Figures 3 and 4 reveal the influence of the mean effective pressure on the predetermined boundary conditions for the thermally stressed surface of the combustion chamber (S1) (Figure 7a), while Figures 5 and 6 provide the corresponding graph for the surface that experiences less thermal load (S2) (Figure 7b).

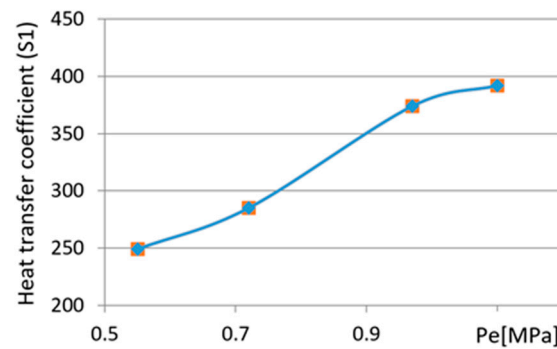


Figure 3. Influence of the mean effective pressure on the predetermined boundary conditions (Heat transfer) for the thermally stressed surface of the combustion chamber (S1).

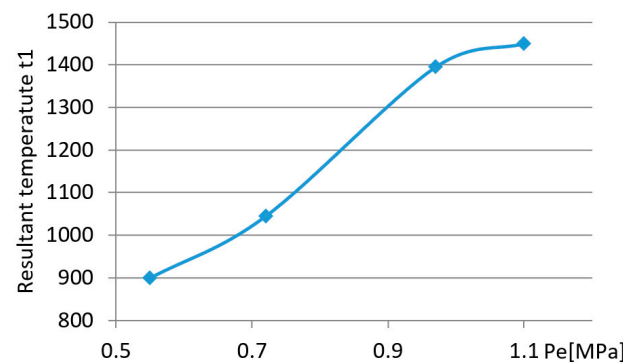


Figure 4. Influence of the mean effective pressure on the predetermined boundary (Resultant temperature) conditions for the thermally stressed surface of the combustion chamber (S1).

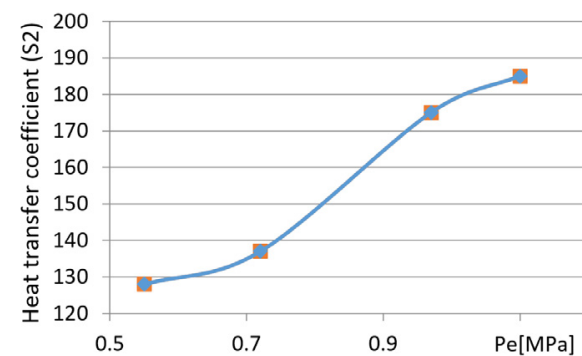


Figure 5. Influence of the mean effective pressure on the predetermined boundary conditions (Heat transfer) for the thermally stressed surface of the combustion chamber (S2).

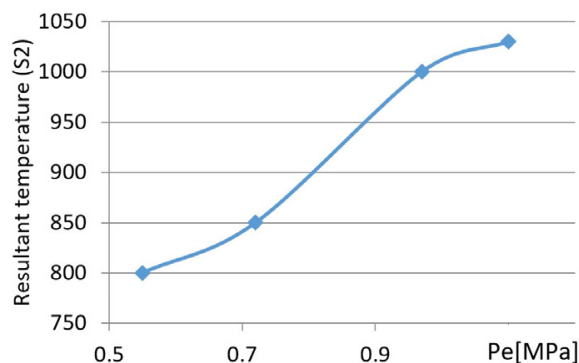


Figure 6. Influence of the mean effective pressure on the predetermined boundary conditions (Resultant temperature) for the thermally stressed surface of the combustion chamber (S2).



Figure 7. Setting boundary conditions across the combustion chamber surface area: (a) Surface 1; (b) Surface 2.

The temperature distribution within the cylinder head is easily affected by the heat exchange parameters across the combustion chamber surfaces. The heat exchange is defined by the average resultant temperature of the hot gases and the heat transfer coefficient, both of which serve as third-kind boundary conditions [7]. The impact of the engine load on the boundary condition values is clearly illustrated in Figures 3 and 4. It appears that the trends observed in the curves for the two parameters (temperature and heat transfer coefficient) demonstrate a consistent pattern across different surfaces.

The temperature field generated from the numerical analysis, based on the experimental research, yields an extensive temperature distribution that enables the calculation of temperatures at any selected point. The variations in temperature throughout the volume of the component are depicted in Figures 8 and 9.

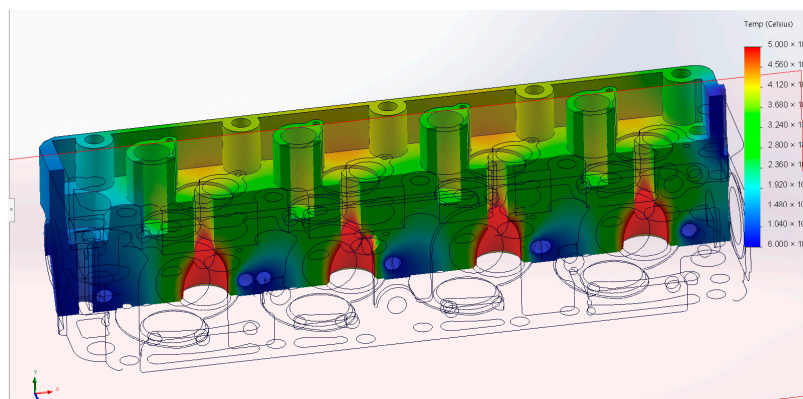


Figure 8. Cut through the exhaust channels in the valve area.

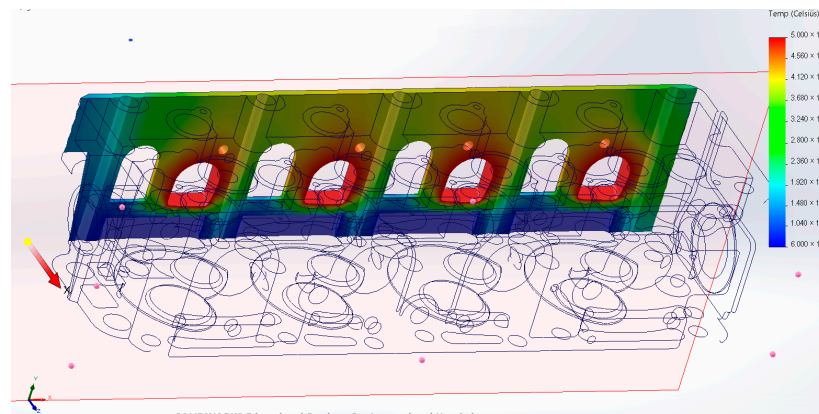


Figure 9. Section of the exit of the exhaust channels.

3. Conclusions

This study presents a novel hybrid theoretical–experimental methodology for comprehensive thermal analysis of cylinder heads operating on gasoline–ethanol blends, addressing the critical challenge of predicting temperature distributions in engines using alternative renewable fuels. The primary scientific contribution lies in developing and validating a systematic approach that combines limited experimental temperature measurements with finite element modeling to generate complete three-dimensional temperature fields, thereby overcoming the inherent limitations of purely experimental investigations.

The methodology demonstrates exceptional accuracy, with numerical predictions deviating from experimental measurements by only 0.09% to 7.03%, and most deviations remaining below 1.5%. For the tested gasoline–E20 blend at 3000 min^{-1} and 30% throttle opening (effective power range of 19.20–38.40 kW), the iterative determination of third-kind boundary conditions successfully established quantitative relationships between engine load and thermal parameters. Specifically, the heat transfer coefficient ranged from 249 to $392 \text{ W/m}^2\text{K}$, while resultant gas temperatures varied between $800 \text{ }^\circ\text{C}$ and $1450 \text{ }^\circ\text{C}$, both correlating strongly with mean effective pressure (0.55–1.10 MPa).

The validated model enables prediction of temperatures at any location within the cylinder head, providing critical insights for thermal management when transitioning to renewable fuel blends. The integration of experimentally measured temperatures as first-kind boundary conditions, combined with the iterative refinement of convective heat transfer parameters as third-kind boundary conditions, establishes a robust and reproducible framework applicable to various engine configurations and operating conditions.

Future research should focus on extending this methodology to higher ethanol concentrations and other biofuel blends to establish comprehensive design guidelines for alternative fuel engines. Investigation of transient thermal behavior during dynamic load variations would provide valuable insights into thermal fatigue mechanisms. Additionally, coupling the thermal model with mechanical stress analysis would enable holistic assessment of component durability under combined thermo-mechanical loading. Experimental validation across multiple engine types and geometries would further enhance the generalizability of the approach, while integration with real-time combustion simulation could enable predictive optimization of cooling systems for next-generation sustainable powertrains.

Author Contributions: Conceptualization, D.P. and S.I.; methodology, D.P. and S.I.; software, S.I.; validation, D.P. and S.I.; formal analysis, D.P.; investigation, D.P. and S.I.; resources, D.P.; data curation, D.P. and S.I.; writing—original draft preparation, D.P. and S.I.; writing—review and editing,

S.I.; visualization, D.P. and S.I. All authors have read and agreed to the published version of the manuscript.

Funding: The present document was supported with the financial assistance of the Project 2025-RU-02 funded by the Scientific Research Fund of the University of Ruse.

Institutional Review Board Statement: Not applicable.

Informed Consent Statement: Not applicable.

Data Availability Statement: The original contributions presented in this study are included in the article. Further inquiries can be directed to the corresponding authors.

Conflicts of Interest: The authors declare no conflict of interest.

References

1. Petkov, D.; Belchev, S.; Yordanov, K. Experimental study into the effect of the addition of fuels from renewable sources on the thermal state of body parts in spark ignition engines, Transport, ecology, sustainable development. *AIP Conf. Proc.* **2024**, *3104*, 020016.
2. Iliev, S. A Comparison of Ethanol, Methanol, and Butanol Blending with Gasoline and Its Effect on Engine Performance and Emissions Using Engine Simulation. *Processes* **2021**, *9*, 1322. [[CrossRef](#)]
3. Zhang, Y.; Yan, Y.; Yang, R.; Wang, Q.; Zhang, B.; Gan, Q.; Liu, Z.; Fu, J. Study of in-cylinder heat transfer boundary conditions for diesel engines under variable altitudes based on the CHT model. *Front. Energy Res.* **2022**, *10*, 828215. [[CrossRef](#)]
4. Li, Y.; Kong, S.C. Coupling conjugate heat transfer with in-cylinder combustion modeling for engine simulation. *Int. J. Heat Mass Transf.* **2011**, *54*, 2467–2478. [[CrossRef](#)]
5. Wróbel, R.; Łoza, L.; Haller, P.; Włostowski, R. The effect of fuel mixture on engine vibrations. *Combust. Engines* **2019**, *177*, 136–138. [[CrossRef](#)]
6. Hu, L.; Yang, J.; Yu, Y.; Dong, F. Analysis and Optimisation of Thermo-Mechanical Coupling Load of Cylinder Head Considering Fluid-Structure Interaction for a Marine High-Power Diesel Engine. *Energies* **2020**, *13*, 3597. [[CrossRef](#)]
7. Zhao, P.C.; Li, Z.; Shang, Z.; Wang, J.F. Experimental study on surface roughness of fused deposition based on Taguchi method. *Exp. Technol. Manag.* **2020**, *3*, 162–164. (In Chinese)

Disclaimer/Publisher's Note: The statements, opinions and data contained in all publications are solely those of the individual author(s) and contributor(s) and not of MDPI and/or the editor(s). MDPI and/or the editor(s) disclaim responsibility for any injury to people or property resulting from any ideas, methods, instructions or products referred to in the content.